Molecular Microbiology (2014) 91(1), 185–197 ■
doi:10.1111/mmi.12454
First published online 20 November 2013

Differential roles for the Co^{2+}/Ni^{2+} transporting ATPases, CtpD and CtpJ, in *Mycobacterium tuberculosis* virulence

Daniel Raimunda,[1†] Jarukit E. Long,[2†] Teresita Padilla-Benavides,[1] Christopher M. Sassetti[2,3] and José M. Argüello[1*]
[1]*Department of Chemistry and Biochemistry, Worcester Polytechnic Institute, Worcester, MA 01609, USA.*
[2]*Department of Microbiology and Physiological Systems, University of Massachusetts Medical School, Worcester, MA 01655, USA.*
[3]*Howard Hughes Medical Institute, Chevy Chase, MD 20815, USA.*

Summary

The genome of *Mycobacterium tuberculosis* encodes two paralogous P_{1B4}-ATPases, CtpD (*Rv1469*) and CtpJ (*Rv3743*). Both proteins showed ATPase activation by Co^{2+} and Ni^{2+}, and both appear to be required for metal efflux from the cell. However, using a combination of biochemical and genetic studies we found that these proteins play non-redundant roles in virulence and metal efflux. CtpJ expression is induced by Co^{2+} and this protein possesses a relatively high turnover rate. A *ctpJ* deletion mutant accumulated Co^{2+}, indicating that this ATPase controls cytoplasmic metal levels. In contrast, CtpD expression is induced by redox stressors and this protein displays a relatively low turnover rate. A *ctpD* mutant failed to accumulate metal, suggesting an alternative cellular function. *ctpD* is cotranscribed with two thioredoxin genes *trxA* (*Rv1470*), *trxB* (*Rv1471*), and an enoyl-coA hydratase (*Rv1472*), indicating a possible role for CtpD in the metallation of these redox-active proteins. Supporting this, *in vitro* metal binding assays showed that TrxA binds Co^{2+} and Ni^{2+}. Mutation of *ctpD*, but not *ctpJ*, reduced bacterial fitness in the mouse lung, suggesting that redox maintenance, but not Co^{2+} accumulation, is important for growth *in vivo*.

Introduction

Upon infection, *Mycobacterium tuberculosis* replicates within a phagosome-like compartment of the host macrophage (Aderem and Underhill, 1999; Flynn and Chan, 2001; Vergne *et al.*, 2004). Transition metal homeostasis (namely $Cu^{+/2+}$, Zn^{2+}, $Fe^{2+/3+}$and Mn^{2+}) can alter the outcome of this interaction by numerous mechanisms (Forbes and Gros, 2001; Argüello *et al.*, 2011; Hood and Skaar, 2012; Rowland and Niederweis, 2012). Increased Cu^{+} and Zn^{2+} and decreased Fe^{2+} concentrations have been described in phagosomes of interferon-gamma-activated macrophages (Wagner *et al.*, 2006). These alterations, in conjunction with the activation of the phagosomal inducible nitrogen oxide synthase (iNOS) and NADPH oxidase, lead to bacterial clearance (Flynn and Chan, 2001; Vergne *et al.*, 2004). The pathogen adapts to this environment through the use of specific metal transporters. Transition metals are essential micronutrients, as they are cofactors in bacterial metalloenzymes necessary for various metabolic processes and coping with redox stress. As a result metal importers are required for bacterial virulence in a number of systems (Forbes and Gros, 2001; Argüello *et al.*, 2011; Botella *et al.*, 2011; Rowland and Niederweis, 2012; Padilla-Benavides *et al.*, 2013). However, at high concentrations these metals can also be cytotoxic, and bacterial efflux systems are equally important for growth in the host environment. Consequently, *M. tuberculosis* infection is dependent on maintaining appropriate transition metal homeostasis.

The *M. tuberculosis* genome possesses an unusually high number of heavy metal transporting P_{1B}-type ATPases.[1] Members of this family of proteins are characterized by a highly conserved core protein structure and a common mechanism of transport (Argüello *et al.*, 2007; 2011). These can be classified into distinct subgroups, clustered by conserved transmembrane metal binding sites (TM-MBS) and consequent metal specificity (Argüello, 2003). P_{1B}-ATPases export cytosolic transition metals as part of metal excess responsive systems, and control cellular metal quotas (Raimunda *et al.*, 2011). Moreover, emerging new data suggest that some P_{1B}-ATPases are part of the redox tolerance machinery of intracellular pathogens, as they participate in the assembly of membrane and secreted redox metalloenzymes (González-Guerrero *et al.*, 2010; Argüello *et al.*, 2011;

Accepted 4 November, 2013. *For correspondence. E-mail arguello@wpi.edu; Tel. (+1) 508 831 5326; Fax (+1) 508 831 4116. †Both authors contributed equally to this work.

[1]For simplicity P-type ATPases will be referred as P-ATPases, P_{1B}-ATPases, etc.

Osman *et al.*, 2013; Padilla-Benavides *et al.*, 2013). These represent a novel function for metal transporters; i.e., they are also part of metalloprotein assembly systems. More importantly, this has notable implications for the conceptual development of metal homeostasis models. This is, transition metals although not free are transported to specific target metalloproteins that from a system perspective operate as metal pool/compartments. The identification of additional examples, in particular with novel and unique metal specificities, validates the general importance of this mechanistic strategy.

The involvement of *M. tuberculosis* P_{1B}-ATPases CtpV (Rv0969) and CtpC (Rv3270) in Cu^{+} and Mn^{2+} homeostasis and virulence has been shown (Ward *et al.*, 2010; Botella *et al.*, 2011; Padilla-Benavides *et al.*, 2013). In addition, a previous genomic analysis directed to identify genes essential for *M. tuberculosis* growth during infection showed the requirement of *ctpD* (*Rv1469*) for *in vivo* survival fitness (Sassetti and Rubin, 2003). CtpD is a member of the Co^{2+}/Ni^{2+}-transporting P_{1B4}-ATPase subgroup (Rutherford *et al.*, 1999; Argüello, 2003; Zielazinski *et al.*, 2012; Raimunda *et al.*, 2012a). Characterization of the *M. smegmatis* homologue (*MSMEG_5403*) showed that it transports Co^{2+} and Ni^{2+} and its transcription was induced by Co^{2+} (Raimunda *et al.*, 2012a). In agreement with this, mutations in *M. smegmatis* Co^{2+}-ATPase led to an increase in intracellular Co^{2+} and Ni^{2+} levels. Additionally, an increase in susceptibility to these metals was observed (Raimunda *et al.*, 2012a). While maintaining cytoplasmic Co^{2+} and Ni^{2+} levels appears as a simple parsimonious role for this subtype of ATPases, this model is complicated by the presence of two homologous P_{1B4}-ATPase coding genes, *ctpD* and *ctpJ*, in several Mycobacterium species including *M. tuberculosis* (Fig. 1A and B). The presence of two paralogous P_{1B4}-ATPases was also observed in *Gramella forsetii*, *Oligotropha carboxidovorans OM5* and *Xanthobacter autotrophicus* (Raimunda *et al.*, 2012a). All these proteins present a large cytoplasmic ATP binding and hydrolysis domains and six transmembrane fragments (TM) containing metal binding residues S in TM4, and HEXXT in TM6 (Argüello, 2003; Zielazinski *et al.*, 2012; Raimunda *et al.*, 2012a).

CtpD and CtpJ homologues from various mycobacteria are closely related at the primary sequence level (Fig. 1A). However, the genes flanking *ctpD/J* homologues are distinct and this genomic context can be used to assign orthology (Fig. 1B and C). The Co^{2+} sensing transcriptional regulator *nmtR* is always upstream of *ctpJ* orthologues. *nmtR* is a member of the ArsR-SmtB family of transcriptional repressors (Cavet *et al.*, 2002). The *ctpD* orthologues are found together with two thioredoxins – *trxA* (*Rv1470*) and *trxB* (*Rv1471*) – and a putative enoyl-CoA hydratase (*Rv1472*) coding genes downstream (Fig. 1C). Unlike TrxB and TrxC, *in vitro* functional studies have shown that TrxA has an unusual low redox potential and is not functional in the presence of *M. tuberculosis* thioredoxin reductase (TrxR) (Akif *et al.*, 2008). Although bioinformatics analysis suggests that *ctpD* transcription is monocistronic (http://www.tbdb.org/), it is notable that *trxA* is always present in the same position next to *ctpD* and is absent in all *Mycobacterium* species missing the *ctpD* homologue. Adding to these correlations, a proteomic study combining cellular fractionation and 2D-LC MS/MS showed the colocalization of CtpD, TrxA and the enoyl-CoA-hydratase in the membrane fraction (Mawuenyega *et al.*, 2005).

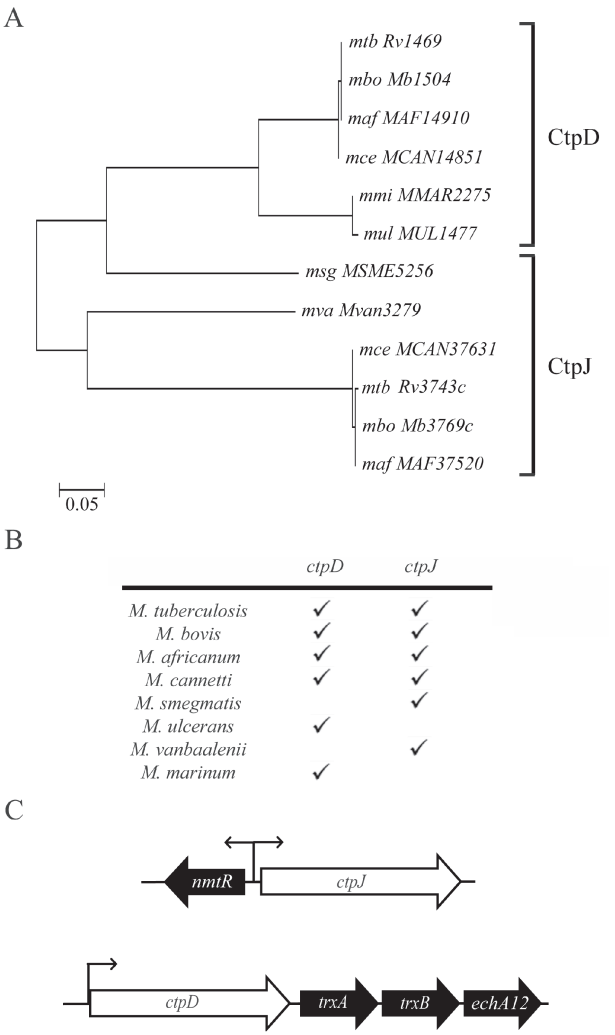

Fig. 1. *M. tuberculosis* genome contains two P_{1B4}-ATPases codifying genes.
A. Rooted tree of mycobacterial P_{1B4}-ATPases obtained from genome-sequenced organisms.
B. Table list describing mycobacterial organisms having *ctpD* and *ctpJ* homologues (check marks indicate the presence of the paralogous gene in that organism).
C. Genetic environment of *M. tuberculosis ctpJ* and *ctpD*; arrows represent the DNA regulatory regions.

Considering the different physiological functions observed in homologous P_{1B}-ATPases (González-Guerrero *et al.*, 2010; Argüello *et al.*, 2011; Osman *et al.*, 2013; Padilla-Benavides *et al.*, 2013), the presence of CtpD and CtpJ in *M. tuberculosis* presents a unique opportunity to demonstrate the broad application of a strategy to employ pairs of metal transporters with similar specificity but different kinetics characteristics, to transport metal to different targets. This general model was tested in comparative *in vivo* and *in vitro* analyses. *In vivo* experiments confirmed the requirement of *ctpD*, but not *ctpJ*, for virulence. Biochemical analysis showed identical metal specificity and transport direction for both ATPases, although they work at different rates. These biochemical characteristics were in agreement with cellular metal accumulation assays and expression profiles under different stress conditions. The data suggest that while CtpJ is responsible for maintaining Co^{2+} cytoplasmic level; CtpD plays a unique role in redox stress response and adapting to the host environment. Furthermore, the cotranscription of CtpD with thioredoxins, their previously demonstrated colocalization, and the specific binding of Co^{2+} to TrxA, suggest that CtpD participates in the metallation of cobaloproteins.

Results

CtpD and CtpJ transport Co^{2+} *and* Ni^{2+} *at different rates*

M. tuberculosis CtpD and CtpJ sequences contain conserved amino acids present in homologous proteins that are selective for Co^{2+} and Ni^{2+} transport (Zielazinski *et al.*, 2012; Raimunda *et al.*, 2012a). P_{1B}-ATPases couple substrate transport across membranes to ATP hydrolysis following the Albers-Post E1/E2-like mechanism (Argüello *et al.*, 2007). Both proteins were expressed in *E. coli* and affinity purified (Fig. 2A), to confirm their metal specificity and analyse their enzymatic characteristics. Protein preparations were incubated with TEV protease and then pretreated with chelating agents before metal dependent ATP hydrolysis was measured (Raimunda *et al.*, 2012a). It is important to note that P_{1B4}-ATPases lack amino- and carboxyl-terminus MBDs (N-, C-MBD) (Argüello, 2003) and that treatment of the protein with TEV protease removes the $(His)_6$-tag used during in enzyme purification (Fig. 2A). Co^{2+} and Ni^{2+} activated CtpD and CtpJ ATPase activity in the μM range (Fig. 2B and C). Other transition metals such as Zn^{2+}, $Cu^{+/2+}$, Mn^{2+} and Fe^{2+} in concentrations ranging from nM to mM failed to activate the enzyme (data not shown). Importantly, CtpD showed a fourfold lower V_{max} compared with CtpJ in presence of either substrate. This was also matched by slightly higher affinity of CtpD for the metal when compared with CtpJ. The V_{max} value for both metals observed for CtpJ, resembles the biochemical behaviour of *M. smegmatis* Co^{2+}-ATPase that we desig-

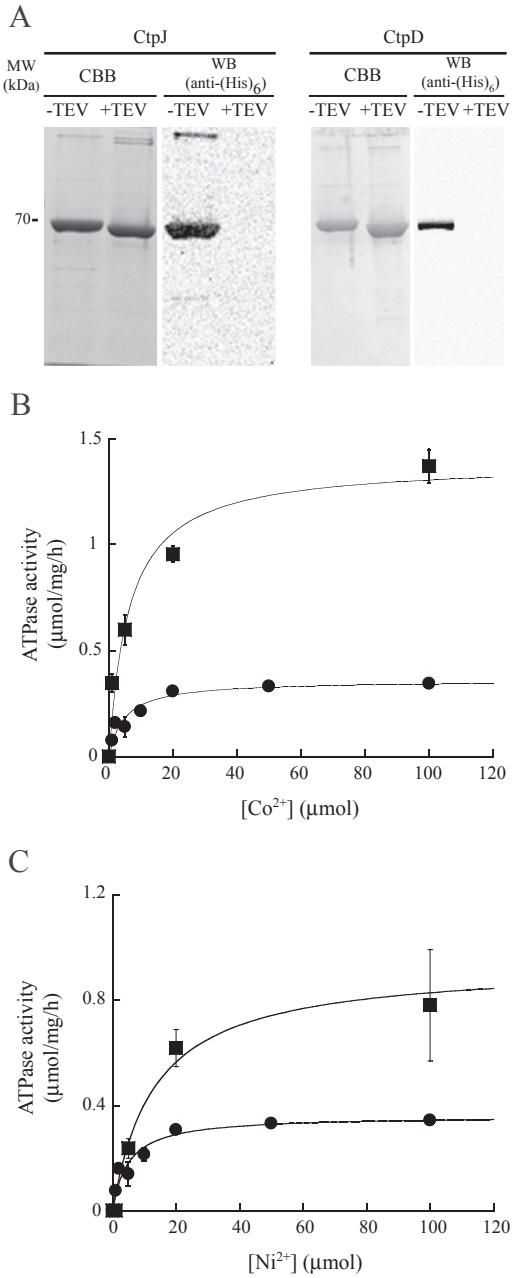

Fig. 2. CtpD and CtpJ are Co^{2+}/Ni^{2+}-ATPases with different transport kinetics. (A) Preparations of Ni-NTA purified CtpD and CtpJ analysed by Coomassie brilliant blue (CBB) and Western blot (WB) using anti-$(His)_6$ tag antibody. (B) Co^{2+} and (C) Ni^{2+}-dependent ATPase activity for CtpD (•) and CtpJ (•). Curves of ATPase activity versus metal concentrations were fit to $v = V_{max}[metal]/([metal] + K_{1/2})$. Kinetic parameters obtained with Co^{2+} for CtpD and CtpJ were $V_{max} = 0.35 \pm 0.03$ μmol mg^{-1} h^{-1}, $K_{1/2} = 4.83$ μM ± 1.4 and $V_{max} = 1.38 \pm 0.12$ μmol mg^{-1} h^{-1}, $K_{1/2} = 6.3 \pm 2.2$ μM respectively. Kinetic parameters with Ni^{2+} for CtpD and CtpJ were $V_{max} = 0.36 \pm 0.02$ μmol mg^{-1} h^{-1}, $K_{1/2} = 4.90 \pm 1.18$ μM and $V_{max} = 0.94 \pm 0.05$ μmol mg^{-1} h^{-1}, $K_{1/2} = 13.23 \pm 2.80$ μM respectively. The reported standard errors for V_{max} and $K_{1/2}$ are asymptotic standard errors reported by the fitting software KaleidaGraph (Synergy). Data are mean ± SE ($n = 3$).

Table 1. Metal binding stoichiometry of His-less CtpD and CtpJ.

	Co^{2+} protein molar ratio[a]		Ni^{2+} protein molar ratio[a]	
Protein	No vanadate	1.5 mM vanadate	No vanadate	1.5 mM vanadate
CtpD	1.08 ± 0.14	0.35 ± 0.02	1.04 ± 0.05	0.38 ± 0.08
CtpJ	1.06 ± 0.27	0.05 ± 0.01	0.92 ± 0.13	0.28 ± 0.03

a. Stoichiometry was estimated as moles metal : moles CtpD. Metal content in protein was determined by furnace AAS.

nate as its orthologue (Fig. 1). The different biochemical kinetics (low versus high transport rate of CtpD versus CtpJ), suggests that while CtpJ might control the cytosolic metal levels, CtpD could be required for additional physiological functions, as seen with other P_{1B1}-ATPases (González-Guerrero *et al*., 2010; Raimunda *et al*., 2011; Osman *et al*., 2013).

CtpD and CtpJ bind cytoplasmic metals

Previous reports on P_{1B4}-ATPases have shown that these enzymes drive the efflux of cytoplasmic Co^{2+} (Rutherford *et al*., 1999; Raimunda *et al*., 2012a). The binding of the metal substrate to the TM-MBS facing the intracellular side is a well-known requisite for ATP hydrolysis by P_{1B}-ATPases (Argüello *et al*., 2007; Raimunda *et al*., 2011). Nevertheless, it can be argued that CtpD or CtpJ might drive Co^{2+}/Ni^{2+} influx and ATP hydrolysis is associated with the efflux of an alternative substrate. This would imply Co^{2+}/Ni^{2+} binding to CtpD or CtpJ in the E2 conformation, i.e., exposing the TM-MBS to the extracellular space. Vanadate stabilizes P-ATPases in E2 conformation (Pick, 1982; Eren and Arguello, 2004). Thus, to evaluate the direction of transport the metal binding of Co^{2+} and Ni^{2+} to CtpD and CtpJ was measured in the absence or presence of vanadate. Incubation of each $(His)_6$-less protein with the metals in a molar ratio 1:10 showed a TM-MBS binding stoichiometry of approximately 1:1 molar ratio in agreement with previous reports (Zielazinski *et al*., 2012; Raimunda *et al*., 2012a) (Table 1). This binding was largely abolished in the presence of 1.5 mM vanadate. The inhibition of metal binding observed in both proteins can be mechanistically explained considering the displacement of the E1/E2 equilibrium towards the E2 state (TM-MBS exposed to the extracellular side) preventing binding to the E1 form. Based on these data, we conclude that both proteins drive the efflux of the cytoplasmic substrate.

Deletion of ctpD and ctpJ cause opposing alterations in cellular Co^{2+} *levels*

Previously described P_{1B}-ATPases have been mostly associated with maintaining cytoplasmic transition metal levels (Argüello *et al*., 2007; 2011; Osman and Cavet, 2008). However, in the human opportunistic pathogen *Pseudomonas aeruginosa*, the two paralogous genes coding for Cu^{+} transporting ATPases show no redundancy in their functional roles. One gene is involved in Cu^{+} homeostasis (CopA1) while the other participates in metalloprotein biogenesis (CopA2) (González-Guerrero *et al*., 2010). Considering the possibility of similar alternative roles for *M. tuberculosis* P_{1B4}-ATPases, their involvement in maintaining cellular metal quotas was tested. Wild-type, single *ctpD::hyg* and *ctpJ::hyg* mutants, and the double mutant *ctpD-ctpJ::hyg* strains were challenged by supplementing 7H9-OADC media with various metals and the resulting cellular metal levels were determined. A significant decrease of Co^{2+} content was observed in the *ctpD::hyg* mutant, whereas Co^{2+} accumulated in *ctpJ::hyg* and *ctpD-ctpJ::hyg* double mutant strains when compared with the wild-type (Fig. 3A). Complemented mutant strains showed metal contents similar to those of wild-type cells. No significant differences were observed in Ni^{2+} or Cu^{2+}-challenged cells (Fig. 3B and C). These results, together with the biochemical kinetic parameters observed in the purified preparations of CtpJ (Fig. 2B), support the hypothesis that CtpJ is responsible for maintaining cytoplasmic Co^{2+} (but not Ni^{2+}) levels. CtpD appears to have an alternative role since deletion of the coding gene does not lead to an increase but rather a decrease in cytoplasmic Co^{2+} level. As shown below this is likely due to a compensatory increase of *ctpJ* expression in the *ctpD* mutant. It is also notable that CtpD is not able to complement the *ctpJ* defect probably because of its slow turnover rate. Additional experiments exploring the tolerance of *ctpD* and *ctpJ* mutant cells to Co^{2+}, Ni^{2+}, Cu^{2+} and Zn^{2+} showed no differences between these and the wild-type strain (Fig. S1) .

Expression of ctpD and ctpJ is induced by different stressors

M. tuberculosis manages to survive in the hostile phagosomal environment through to its ability to adapt to changes in pH, transition metal bioavailability, redox stress and nutritional starvation (Ehrt and Schnappinger, 2009; Rowland and Niederweis, 2012). Toward elucidat-

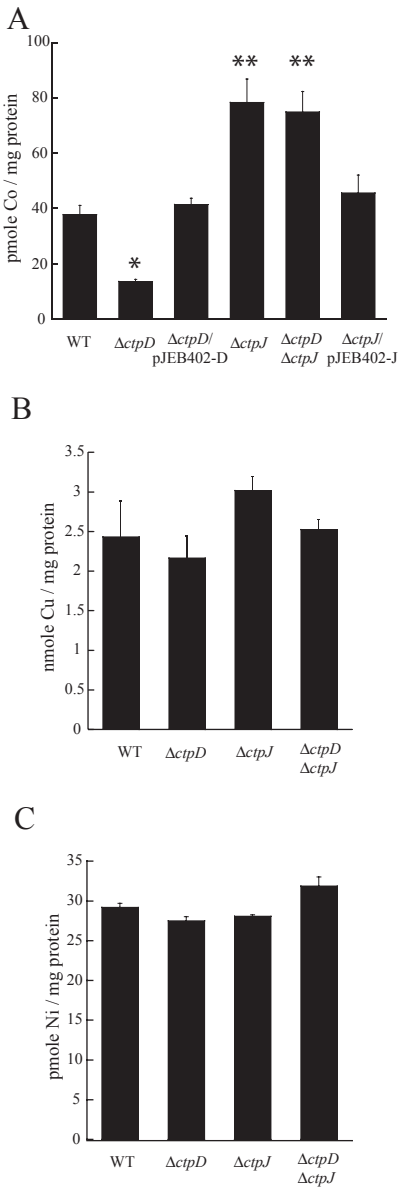

Fig. 3. Metal accumulation in *M. tuberculosis ctpD::hyg* (Δ*ctpD*) and *ctpJ::hyg* (Δ*ctpJ*) mutant strains. Log-phase cell cultures grown in 7H9-OADC media were supplemented with (A) 100 nM Co^{2+}, (B) 3 μM Cu^{2+} or (C) 1 μM Ni^{2+} for 2 h. Data represent mean ± SE ($n = 3$). *$P < 0.01$ and **$P < 0.05$ versus wild-type.

ing the mechanism of *ctpD* participation in the infection process, its expression under stress conditions present in the phagosome and upon exposure to various metals was studied. Sublethal concentrations for Co^{2+}, Ni^{2+} and Zn^{2+} were chosen from metal sensitivity assays (Fig. S1). None of the tested metals induced *ctpD* expression (Fig. 4A). On the other hand, in a similar manner to the *M. smegmatis* orthologue, expression of *ctpJ* in *M. tuberculosis* was induced by the presence of Co^{2+} (Fig. 4B) (Cavet *et al.*, 2002; Raimunda *et al.*, 2012a). Addition of Ni^{2+} to the media did not induce the transcription of *ctpD* or *ctpJ* (Fig. 4A and B). Among a battery of tested redox stressors, nitroprusside and potassium cyanide (KCN) increased *ctpD* expression 10- and 7-fold respectively (Fig. 4A). Nitroprusside, triclosan and tert-butyl hydroperoxide (TBHP) also led to induction of *ctpJ* transcription, although these were smaller than the induction by Co^{2+} (Fig. 4B).

The lack of *ctpD* induction by metals might be a consequence of the media used, as 7H9 contains significant amounts of Cu^{2+} and Zn^{2+}. Similarly, lack of *ctpJ* Ni induction could be due to Ni^{2+} presence. Therefore, we tested the response to Cu^{2+}, Zn^{2+}, Co^{2+} and Ni^{2+} of *ctpD* and *ctpJ* transcription in cells grown in Sauton's media treated with Chelex. This treatment decreased metal levels to sub-nM concentrations as measured by AAS (not shown). None of the metals tested induced *ctpD* transcription (Fig. 4C). Unexpectedly, its transcription was decreased by Zn^{2+}. Like in 7H9 media, *ctpJ* was induced only by Co^{2+} (Fig. 4D). Since CtpD and CtpJ are highly homologous and are both capable of binding and transporting Co^{2+}, a compensatory induction of one ATPase in a mutant lacking the other might be hypothesized. No induction of *ctpD* was observed in the *ctpJ::hyg* mutant strain (relative expression was 0.55 ± 0.01 fold, relative to that observed in the wild-type cells). Alternatively, when *ctpJ* expression was analysed in the *ctpD::hyg* cells a 3.6 ± 0.6 fold induction was observed (Fig. 4E). This induction of *ctpJ* in the *ctpD::hyg* mutant strain likely explains the decrease in intracellular Co^{2+} observed in these cells (Fig. 3A).

ctpD is cotranscribed with thioredoxin A, B and an enoyl-CoA hydratase under reactive nitrogen species (RNS) stress

The described data support the role of CtpD as a Co^{2+}-ATPase distinct from CtpJ, but did not reveal the role of this enzyme. *ctpD's* genetic environment was considered in the search for clues on its role (Fig. 1C). Genetic studies have shown that in *M. tuberculosis ctpD* and *trxA* are under regulation of the stress-responsive sigma factor SigF. *M. tuberculosis sigF* is induced under stress conditions such as nutrient starvation, macrophage infection, or stationary phase entry (Williams *et al.*, 2007). Searching for a molecular/functional link between these genes, we evaluated whether or not *ctpD* is part of a contiguous operon cotranscribed with down-stream genes under stress conditions (Fig. 1C). RNA extracted from cells challenged for 2 h with nitroprusside was reverse-transcribed and the operon was mapped by PCR. Figure 5 shows that *ctpD* is cotranscribed in a single operon together with *trxA*, *trxB* and *echA12*, an enoyl-CoA hydratase, suggesting the participation of these genes in a co-ordinated response.

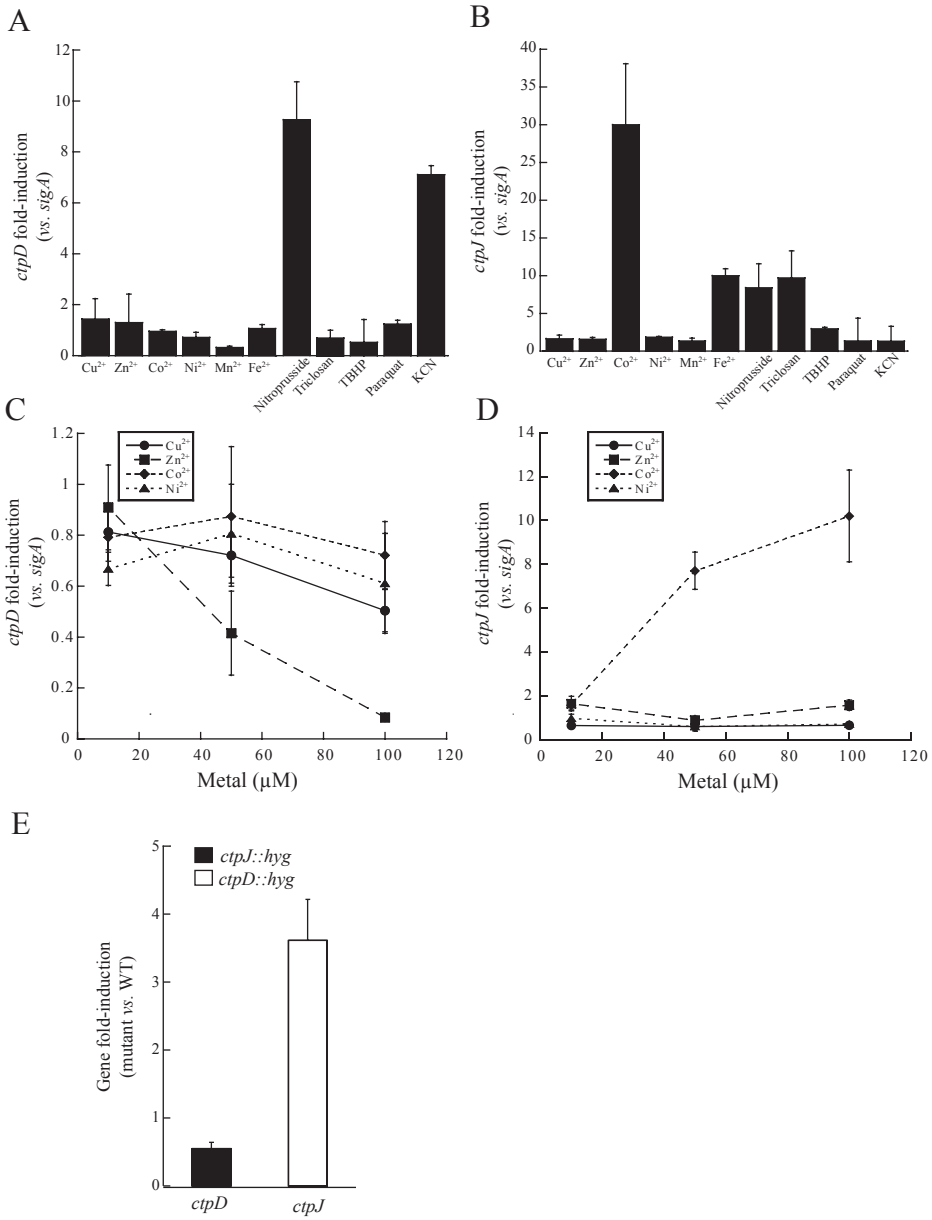

Fig. 4. Transcriptional analysis of *ctpD* and *ctpJ* in *M. tuberculosis*. Log-phase H37Rv *M. tuberculosis* cell cultures grown in 7H9-OADC (A, B, E) or Chelex-treated Sauton's media (C, D) were supplemented or not, with the indicated metals and redox stressors for 2 h. RNA was extracted and gene expression analysed for (A, C) *ctpD* or (B, D) *ctpJ* transcriptional induction. (E) *ctpD* and *ctpJ* fold-induction analysed in *ctpJ::hyg* (black bar) or *ctpD::hyg* (white bar) strains respectively. Data represent mean ± SE ($n = 3$).

TrxA binds specifically Co^{2+} *and* Ni^{2+}

The cotranscription of *trxA* and *ctpD* together with their colocalization (Mawuenyega *et al.*, 2005), and the low turnover rate of CtpD suggest that TrxA could be a CtpD's client protein in the extracellular side of the membrane. In this way TrxA would be capable of accepting Co^{2+}/Ni^{2+} as a metal chaperone or a redox buffer/operator. To test this, metal binding to heterologously expressed and purified TrxA was assayed. Prior to this, the $(His)_6$-tag used for purification was removed from TrxA by TEV treatment (Fig. 6A). TrxA was capable of Co^{2+} and Ni^{2+} binding under reducing conditions with a stoichiometry of 2:1 (Fig. 6B). This binding appeared specific for these metals since the protein could not bind Zn^{2+}.

ctpD is required for the growth of M. tuberculosis *in mouse lung*

Previous whole genome genetic screens suggested that *ctpD* but not *ctpJ* may be required for the growth or

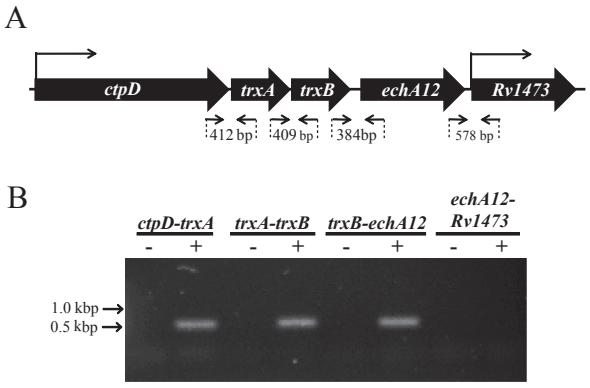

Fig. 5. *ctpD* is cotranscribed with *trxA*, *trxB* and Rv1472 under nitrosative stress. (A) Schematic illustration and (B) representative gel of the *ctpD* operon as determined by RT-PCR using the RNA obtained from *M. tuberculosis* wild-type cells grown under nitrosative stress conditions (1 mM nitroprusside in 7H9-OADC for 2 h). The location of primers (small arrows) and expected size of the amplification product are indicated. '–' and '+' indicate no retro transcribed RNA control and retro transcribed RNA (cDNA) respectively.

survival of *M. tuberculosis* during infection (Sassetti and Rubin, 2003). To verify this prediction, we directly determined the relative fitness of these mutants in a competitive infection assay. Mice were infected with a mixture of wild-type and mutant bacteria and the relative fitness of each strain was estimated by determining the change in ratio (wild-type/mutant) in mouse lungs over time (Fig. 7). Over a 28-day infection the representation of the *ctpD::hyg* mutant decreased by 10-fold. In contrast, the *ctpJ::hyg* strain and the complemented *ctpD::hyg* mutant grew indistinguishably from wild-type *M. tuberculosis*.

Discussion

The P_{1B}-ATPase transition metal transporters are emerging as important determinants of virulence in a variety of intracellular pathogens (Osman *et al.*, 2010; Argüello *et al.*, 2011; Botella *et al.*, 2011; Raimunda *et al.*, 2011; McLaughlin *et al.*, 2012; Padilla-Benavides *et al.*, 2013). Genomes of pathogens frequently contain several P_{1B}-ATPases, with identical metal specificity and direction of transport (Argüello, 2003; Argüello *et al.*, 2011; Osman *et al.*, 2013). Co^{2+} transporting P_{1B4}-ATPases are widely distributed in nature (Rutherford *et al.*, 1999; Argüello, 2003; Zielazinski *et al.*, 2012; Raimunda *et al.*, 2012a). However, only some plants and a few bacterial genera, *M. tuberculosis* among them, possess two P_{1B4}-ATPases. Those present in mycobacteria have been referred as CtpD and CtpJ. Previous genetic screens suggested that these proteins serve non-redundant roles during infection (Sassetti and Rubin, 2003). On the other hand, evidence is emerging supporting distinct roles for Cu^{+}- and Mn^{2+}-ATPases not only in maintaining cytoplasmic metal quotas, but also participating in the assembly of metalloproteins. In this report, we present evidence of the alternative functions played by Co^{2+}-ATPases in mechanisms of metal homeostasis and allocation. In particular, we characterize the functional role CtpD, and its singular importance for *M. tuberculosis* virulence.

Recent biochemical studies of bacterial P_{1B4}-ATPases support their role in Co^{2+} and possibly Ni^{2+} homeostasis (Zielazinski *et al.*, 2012; Raimunda *et al.*, 2012a). *M. tuberculosis* CtpJ and CtpD are structurally homologous to those previously studied. Our results show that both Co^{2+} and Ni^{2+} trigger the CtpD and CtpJ ATPase activity. The apparent substrate affinities and the relative activation by Ni^{2+} and Co^{2+} are similar to those previously described (Zielazinski *et al.*, 2012; Raimunda *et al.*, 2012a). However, metal accumulation experiments performed in

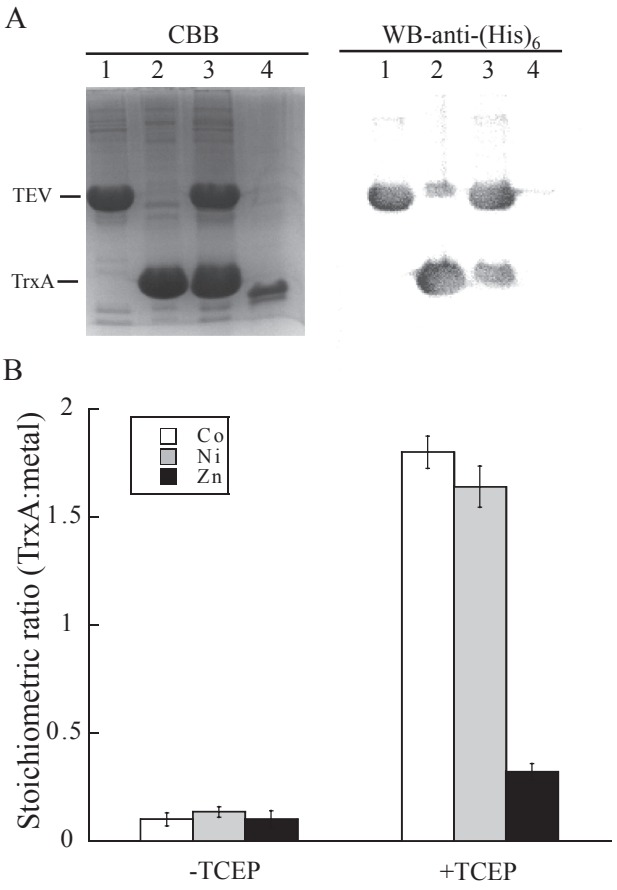

Fig. 6. TrxA binds Co^{2+} and Ni^{2+}.
A. Coomassie brilliant blue (CBB) and immune staining with anti-$(His)_6$ antibody (WB-anti-$(His)_6$) of (1) $(His)_6$-TEV, (2) $(His)_6$-Tev-TrxA, (3) $(His)_6$-Tev-TrxA plus $(His)_6$-TEV at time zero and (4) reverse purified $(His)_6$-less TrxA after 3 hour incubation. Note that Tev refers to the cleavage site and TEV refers to the protease.
B. Co^{2+} (white bars), Ni^{2+} (grey bars) or Zn^{2+} (black bars) binding to $(His)_6$-less TrxA was determined in the presence (+) and absence (–) of TCEP. Data represents the mean ± SE ($n = 3$).

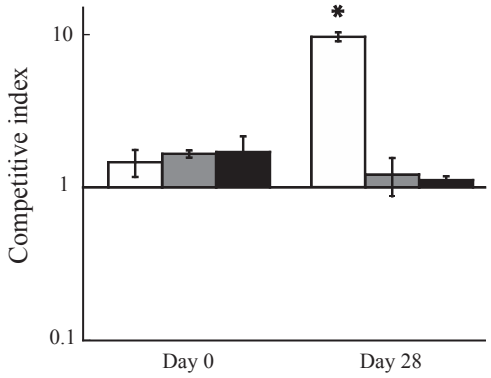

Fig. 7. CtpD is required for proper fitness of *M. tuberculosis* in a mix competition assay. Competitive index of each mutant relative to wild-type H37Rv was measured at 0 and 28 days post infection in mice lungs. White bars, *ctpD::hyg* mutant versus H37Rv; gray bars, *ctpJ::hyg* mutant versus H37Rv; black bars, *ctpD::hyg* mutant complemented with plasmid pJEB402-D versus H37Rv. Data are mean ± SE ($n = 3$). *$P < 0.05$ versus post-infection day 0.

M. smegmatis (Raimunda *et al*., 2012a) and *M. tuberculosis* (this study), as well as induction of gene expression by Co^{2+} but not Ni^{2+} (Rutherford *et al*., 1999; Raimunda *et al*., 2012a), strongly indicate that these enzymes transport Co^{2+} rather than Ni^{2+} *in vivo*. The lack of CtpJ induction by Ni^{2+} appears to be at odds with previous LacZ reporter studies, which concluded that the operator-promoter region of *ctpJ* is driven by NmtR in mycobacterial cells grown with Ni^{2+} (Cavet *et al*., 2002). However, these studies were performed after much longer (20 h versus 2 h) exposure to similar metal levels. It is possible that this harsh condition might be eliciting pleiotropic effects leading to gene induction. Although unlikely, in our experimental conditions, a Ni^{2+} carryover in cells grown in 7H9 media could mask a transcriptional induction in the Chelex-treated Sauton's media.

M. tuberculosis CtpJ maximum activity is comparable to that of the *M. smegmatis* ortholog, although both are much lower (30-fold) than that reported for CoaT from *Sulfitobacter* sp. *NAS-14.1* (Zielazinski *et al*., 2012). However, the high activity of CoaT might be exceptional, as it is much higher than any other reported for a transition metal transporter. The even slower turnover rate of CtpD suggests that this protein might not contribute to maintenance of the cytoplasmic levels of these metals. Metal accumulation experiments support this idea. Co^{2+} accumulated in the *ctpJ::hyg* mutant strain, while the *ctpD::hyg* showed a decrease in Co^{2+} content (the double *ctpD-ctpJ::hyg* mutant showed Co^{2+} levels comparable to the *ctpJ::hyg* mutant). This observation might raise the question of whether CtpD drives metal efflux or influx. Both CtpD and CtpJ, binds the substrate to be exported when intracellular-facing transport sites are available, strongly implying that both act as exporters. Instead, we speculate that the observed compensatory induction of *ctpJ* expression in the *ctpD::hyg* mutant is responsible for the decreased Co^{2+} levels. While *ctpJ* induction might be related to a RNS detoxification-like effect produced by the deletion of *ctpD* (*ctpJ* is induced by nitroprusside), it also results in a higher Co^{2+} exporting capability. This compensatory effect of *ctpD* deletion is reminiscent of the decrease in Cu^{+} content after deletion of Cu^{+}-ATPases likely involved in metallation of cuproproteins rather than maintaining compartmental Cu^{+} levels (Tottey *et al*., 2001; Argüello *et al*., 2011; Raimunda *et al*., 2011).

Surprisingly, the growth of *ctpD::hyg* and *ctpJ::hyg* *M. tuberculosis* strains was not inhibited by Co^{2+}. This could be explained on the basis of the heightened capacity of *M. tuberculosis* cells to sense and respond to increases in the bioavailability of Co^{2+}. It is known that this function is shared by two transcriptional repressors (Cavet *et al*., 2002; Campbell *et al*., 2007). Responses mediated by NmtR lead to *ctpJ* transcriptional induction, while KmtR mediates the induction of *Rv2025c*, a putative cation diffusion facilitator (CDF) transporter (Campbell *et al*., 2007). NmtR responses are observed at high metal concentrations, whereas KmtR has been detected to act with an extremely high-affinity. In this scenario, and with a high metal content in the sensitivity assay, the *Rv2025c* gene product could be responsible for maintaining tolerable cytoplasmic Co^{2+} levels in the absence of CtpJ. While the unique roles of CtpJ and Rv2025c remain unclear, their differential regulation, substrate specificity, or energetic requirements are likely to underlie the retention of both in the genomes of many mycobacterial species.

Stringent and hostile conditions met by *M. tuberculosis* in phagosomes induce expression of genes required for fundamental metabolic tasks, such as detoxification of reactive oxygen species (ROS), RNS, and transition metal homeostasis. To this end, physiological stresses faced by *M. tuberculosis* in phagosomes were mimicked *in vitro* and *ctpD* and *ctpJ* expression levels in wild-type strain were analysed. Among the several stimuli, only nitroprusside and cyanide induced the *ctpD* transcription (Fig. 4A). Both of these compounds inhibit respiratory chain electron flow and might influence *ctpD* expression by altering cellular redox state.

CopA2, a Cu^{+}-transporting ATPase in *P. aeruginosa*, was shown to be part of an operon containing the *cbb3-1* and *cbb3-2* involved in cytochrome *c* oxidase assembly by supplying Cu^{+} to the catalytic site (González-Guerrero *et al*., 2010; Hassani *et al*., 2010). The observed connections between *ctpD* and *trxA* in mycobacteria lead us to analyse the possibility that these genes are part of the same operon and the potential functional link between them. Using RNA obtained from cells grown under nitrosative stress, we determined the cotranscription of *ctpD* with *trxA*, *trxB* and *echA12*. To understand if *M. tubercu-*

losis TrxA is a metalloprotein that could be loaded by an ATPase such as CtpD, we assayed its metal binding capability. Under reducing conditions with TCEP, the protein was able to bind Co^{2+} and Ni^{2+}, but not Zn^{2+}, in a protein : metal ratio of 2:1 (Fig. 6B). Although differential competition for the metal between TCEP and TrxA cannot be discarded, its divalent metal adducts have similarly low stabilities. This, along with the identification of *ctpD*, *trxA* and *echA12* gene products in membrane fractions, suggests a co-ordinated function, perhaps a role in lipid membrane metabolism (Mawuenyega *et al*., 2005). However, the participation of transition metals as cofactors of enoyl-CoA hydratases is unknown (Agnihotri and Liu, 2003) and *trxA* has been reported to be non-functional (Akif *et al*., 2008), although this could be due to inappropriate protein maturation. Interestingly, a recent report identifying virulence factors in *P. aeruginosa* proposed an enoyl-CoA hydratase to be relevant for infection of *Caenorhabditis elegans*. Its participation in a fatty acid synthesis is likely required for membrane signalling and quorum sensing (Feinbaum *et al*., 2012). A similar mechanism might be present in *M. tuberculosis*. The study of these hypothetical links is beyond the scope of the work presented here.

Finally, the requirement of CtpD and CtpJ for *M. tuberculosis* virulence was evaluated in a competition (mutant versus wild-type) infection model. Consistent with previous genomic screens using transposon libraries, our results highlight the importance of *ctpD*, but not *ctpJ*, during *M. tuberculosis* infection (Sassetti and Rubin, 2003). Mixed competition assays are useful in determining relative fitness and have been used to demonstrate indispensability of Zn^{2+} transport systems in *Haemophilus influenza* (Rosadini *et al*., 2011). The lack of CtpJ participation in virulence is not surprising considering that no apparent changes in Co^{2+} (or Ni^{2+}) levels in activated phagosomes have been reported (Wagner *et al*., 2005). So why are *ctpD* mutants attenuated during infection? The decreased levels of Co^{2+} found in the *ctpD* mutant strongly argues against toxicity due to metal accumulation in the bacterial cell. Instead, the putative involvement of CtpD in the response to redox stress in the phagosome might explain why CtpD is required for virulence (Flynn and Chan, 2001; Vergne *et al*., 2004). CtpD's cotranscription with *trxAB* and *echA12* may suggest that CtpD plays a role in activating these proteins through metallation, protecting *M. tuberculosis* from redox stress. CtpD may also play a role in activating other proteins required for growth.

In this study, we have characterized the functional roles of two *M. tuberculosis* P_{1B4}-ATPases and established their requirement for the infection process. CtpJ is in charge of cytosolic Co^{2+} and Ni^{2+} levels and is dispensable for infection. CtpD appears necessary for metallation of secreted proteins and for overcoming redox stress, reflecting its requirement in *M. tuberculosis* to strive in the harsh environmental phagosome conditions. It remains to be elucidated the participation of CtpD in fatty acid synthesis, plasma membrane lipid remodelling, or signalling processes during lung colonization.

Experimental procedures

Recombineering, mutant and complemented strains preparation

Deletion mutants were prepared in the background of the *M. tuberculosis* H37Rv wild-type strain using primers listed in Table 2 according to standard protocols (van Kessel and Hatfull, 2007). For *ctpD* mutation, a 1000 bp fragment corresponding to the 5′ first 500 bp and 3′ last 500 bp of the *ctpD* gene was designed using tuberculist (http://tuberculist.epfl.ch). These regions included 30 bp that flanked upstream and downstream of *ctpD* gene. Additionally, an insertion cassette containing the restriction sites for SpeI-HpaI-AscI was added between the 5′ and 3′ 500 bp regions. The resulting synthesized fragment was then inserted in a HindIII site into a pUC57 expression vector (GenScript), resulting in pEL2a. Vector pKM342 contains a hygromycin resistance (hygR) cassette flanked by SpeI-AscI sites. To insert the hygR cassette in pEL2a, both pEL2a and pKM342 were digested with SpeI-AscI. The 1.2 kbp hygromycin fragment was then ligated into pEL2a, resulting in pEL2b. To generate the deletion mutant of *ctpJ* two 500 bp amplicons corresponding to the 5′ first 400 bp plus 100 bp upstream, and the 3′ last 400 bp plus 100 bp downstream of the *ctpJ* gene were obtained by PCR. These were ligated in pJM1 flanking a hygR cassette resulting in pJM1-J. To generate *ctpD* and *ctpJ* mutants, the resulting 2.2 kbp *ctpD-hygR-ctpD* fragment from digestion of pEL2b with HindIII and the 2.8 kbp *ctpJ-hygR-ctpJ* generated by PCR using as template pJM1-1 plasmid, were both transformed into *M. tuberculosis* H37Rv recombineering strain. Briefly, the *M. tuberculosis* H37Rv recombineering strain bearing plasmid pJV53 was grown till $OD_{600} = 0.7$ and incubated for 18 h with 1 μM isovaleronitrile. The culture was treated with 0.2 M glycine for 8 h before making electrocompetent cells. The recombineering strain was electroporated and selected by hygromycin resistance on 7H10 plates. After 18 days, hygR colonies were isolated and transferred to 2 ml inkwells containing 7H9 media supplemented with 50 μg ml^{-1} hygromycin. To verify the presence of the *ctpD* and *ctpJ* deletion mutation, PCR amplification of the hygR cassette flanked by the N- and C- terminals was performed. The double mutant was obtained as described above for *ctpJ*, although using a cleaned-up hygromycin sensitive *ctpD* mutant as parental strain.

The complementation assay constructs were made by amplifying *M. tuberculosis ctpD* and *ctpJ* from genomic DNA. The resulting PCR fragments were digested and ligated into pJEB402 which confers kanamycin resistance (kanR) resulting in pJEB402-D and pJEB402-J. The ligation reactions were transformed into DH5α cells and the presence of the insert was verified by colony PCR and restriction digests. The plasmids were then purified and transformed into the *ctpJ* and *ctpD M. tuberculosis* mutant strains. Transformants showing kanR were analysed for the presence of *ctpD* and *ctpJ* by PCR.

Table 2. List of primers used in this work.

Name	Sequence	Use
qctpD-F	GCCGCCATCGTCTTGTTG	qPCR of *ctpD*
qctpD-R	GCATCCGGACGAAGCTGATC	qPCR of *ctpD*
qctpJ-F	CGGCATCTGGGTGTACGAA	qPCR of *ctpJ*
qctpJ-R	TGGGTGCTCACTGGGATAC	qPCR of *ctpJ*
qsigAMtb-F	CTCGGTTCGCGCCTACCTCA	qPCR of *sigA*
qsigAMtb-R	GCGCTCGCTAAGCTCGGTCA	qPCR of *sigA*
For-ctpD	ATGACCTTGACCGCTTGTGAAG	Clone *ctpD* + TEV in pBAD
Rev-TEV-D	CGCGGCTTCGGCTGCGCGTAGCAGCGGCGAAAACCTGTATTTTCAGTCC	Clone *ctpD* + TEV in pBAD
For-ctpJ	GTGGCTGTTCGTGAACTCTCTC	Clone *ctpJ* + TEV in pBAD
Rev-TEV-J	CGCTGGCACCGCGCACAGGAGCAGCGGCGAAAACCTGTATTTTCAGTCC	Clone *ctpJ* + TEV in pBAD
For-TrxA	ATGACCACTCGAGACCTCAC	Clone trxA + TEV in pEXP5-CT
Rev-TEV-TrxA	CCTGGAACAAAGACTTCATCCAGCAGCGGCGAAAACCTGTATTTTCAGTCC	Clone trxA + TEV in pEXP5-CT
F-ctpJ-EcoRI	AGCTGAATTCGTGGCTGTTCGTGAACTCTCTC	Clone *ctpJ* in pJEB402 under *mop* promoter regulation
R-ctpJ-HpaI	GACTGTTAACTCACCTGTGCGCGGTGCCAGC	Clone *ctpJ* in pJEB402 under *mop* promoter regulation
prEL4-ctpD forward	ATTCTAGACGATGATTAGCGCGGCCAAC	Clone *ctpD* in pJEB402 under *mop* promoter regulation
prEL6-ctpD reverse	ATGGTACCAGCGTGGGCAACAACTTGAC	Clone *ctpD* in pJEB402 under *mop* promoter regulation
F-5UTR-ctpJ	ACTGGCGGCCGCGACCAAGGTGCAAGTGCTCGCTG	Clone 400 bp upstream *ctpJ* including first 100 bp of the gene
R-5UTR-ctpJ	CAGTACTAGTCCCAACGCATCTCCGACAACGC	Clone 400 bp upstream *ctpJ* including first 100 bp of the gene
F-3UTR-ctpJ	ACTGCTCGAGCGCCCGACACGAAGGTTCCACC	Clone 400 bp downstream *ctpJ* including last 100 bp of the gene
R-3UTR-ctpJ	CAGTGGGCCCAGCGAGCGTCCTCGGTGGACC	Clone 400 bp downstream *ctpJ* including last 100 bp of the gene
For-1469	ACGATCATCGGGTTGGCACG	*ctpD* genetic environment
Rev-1470	GTCAAAGTGTTTCCGCGACG	*ctpD* genetic environment
For-1470	CGAGAAAGATCTGGCCTCG	*ctpD* genetic environment
Rev-1471	CGCTGCAAGCTCTCGTTC	*ctpD* genetic environment
For-1471	GAACGAGAGCTTGCAGCG	*ctpD* genetic environment
Rev-1472	CGCTAAGGCCTCTTTGAGC	*ctpD* genetic environment
For-1472	GATGAACAGCTGCTAGATGC	*ctpD* genetic environment
Rev-1473	CTTCTCCAGATCAGTGAGC	*ctpD* genetic environment

Mice infection

The relative growth rates of *M. tuberculosis* H37Rv wild-type and *ctpD::hyg* and *ctpJ::hyg* mutant strains, were examined *in vivo* competition experiments. Briefly, the two strains were mixed with wild-type H37Rv in approximately 3:1 (wild-type:*ctpD::hyg* or wild-type:*ctpJ::hyg* mutants) ratio (final volume 200 µl), containing 6×10^5 cfu and were inoculated into the tail vein of female C57BL/6J mice. Groups of three mice were sacrificed at indicated time points and the bacterial burden in the lung homogenates were obtained by plating on 7H10 agar medium with or without 100 µg ml^{-1} hygromycin for mutants cfu and total cfu counting respectively. A competitive index was calculated as $(\text{cfu WT/cfu mutant})_{output}/(\text{cfu WT/cfu mutant})_{input}$. Mice were housed under specific pathogen-free conditions and in accordance with the University of Massachusetts Medical School, IACUC guidelines.

Protein expression and purification

cDNA encoding *M. tuberculosis ctpD*, *ctpJ* and *trxA* were amplified using genomic DNA as template and reverse primers that introduced a Tobacco etch virus (TEV) protease site coding sequence at the amplicon 3′ ends. The PCR products were cloned into pBAD-TOPO/His (*ctpD* and *ctpJ*) or pEXP5-CT-TOPO (*trxA*) vector (Invitrogen) that introduce a $(His)_6$-tag at the carboxyl end of the protein. cDNA sequences were confirmed by automated sequence analysis. For CtpD and CtpJ expression the constructs were introduced into *E. coli* LMG194 Δ*copA* cells (Rensing *et al.*, 2000). For protein expression, cells were grown at 37°C in ZYP-505 media supplemented with 0.05% arabinose, 100 µg ml^{-1} ampicillin, and 50 µg ml^{-1} kanamycin (Studier, 2005). Affinity purification of membrane proteins and removal of the $(His)_6$-tag was performed as previously described (Mandal *et al.*, 2002; Raimunda *et al.*, 2012b). Solubilized lipid/detergent micellar forms of CtpD and CtpJ proteins were stored at –20°C in buffer containing 25 mM Tris, pH 8.0, 50 mM NaCl, 0.01% n-dodecyl-β-D-maltopyranoside (DDM) (Calbiochem), and 0.01% asolectin until use. TrxA was expressed in BL21 (DE3)pLysS cells transformed with pEXP5-CT-TrxA following the protocol described previously (Akif *et al.*, 2008). Protein determinations were performed in accordance to Bradford (Bradford, 1976). Protein purity was assessed by Coomassie brilliant blue (CBB) staining of overloaded SDS-PAGE gels and by immunostaining Western blots with rabbit anti-$(His)_6$ polyclonal primary antibody (GenScript) and goat anti-rabbit IgG secondary antibody coupled to horseradish peroxidase (GenScript). Previous to ATPase activity determinations, proteins (1 mg ml^{-1}) were treated with 0.5 mM EDTA and 0.5 mM tetrathiomolybdate (TTM) for 45 min at room temperature. Chelators were removed using Ultra-30 Centricon (Millipore) filtration devices.

ATPase assays

These were performed at 37°C in a medium containing 50 mM Tris (pH 7.4 at RT), 3 mM $MgCl_2$, 3 mM ATP, 0.01% asolectin, 0.01% DDM, 20 mM cysteine, 50 mM NaCl, 2.5 mM DTT, and 10–40 mg ml^{-1} purified protein plus the indicated metal concentrations. DTT was replaced by TCEP to prevent interference with the colorimetric reaction when

Co^{2+} activation was measured. ATPase activity was measured after 10 min incubation and released Pi determined according to Lanzetta *et al*. (1979). ATPase activity measured in the absence of metal was subtracted from plotted values. Curves of ATPase activity versus metal concentrations were fit to $v = V_{max}[metal]/([metal] + K_{1/2})$. The reported standard errors for V_{max} and $K_{1/2}$ are asymptotic standard errors reported by the fitting software KaleidaGraph (Synergy).

Metal binding determinations

Maximum metal binding to isolated CtpD and CtpJ in the presence (1.5 mM) or absence of vanadate was measured as previously described (Raimunda *et al*., 2012a). Ten-micromolar CtpD was incubated for 1 min at 4°C in 50 mM HEPES-NaOH, pH 7.5, 200 mM NaCl, 1 mM TCEP, and 50 μM of $CoCl_2$ or $NiCl_2$. After incubation, excess metal was removed by size exclusion using Sephadex G-25 columns (GE Healthcare). Eluted protein was acid digested with 1.25 ml HNO_3 (trace metal grade) for 1 h at 80°C and then overnight at 20°C. Digestion was concluded by addition of 0.25 ml of 30% H_2O_2 and dilution to 3 ml with water. Metal binding to TrxA was similarly determined except that Sephadex G-10 columns were used to remove metal excess. Metal content in digested samples was measured by furnace atomic absorption spectroscopy (AAS; Varian SpectrAA 880/GTA 100). Background metal level in control samples lacking protein was < 10% of those observed in protein containing samples.

Metal content analysis

M. tuberculosis H37Rv wild-type, the single *ctpD::hyg* and *ctpJ::hyg*, and the double *ctpD-ctpJ::hyg* deletion mutants and complemented strains were grown to the late exponential phase and incubated in the presence or absence of 1 μM $CoCl_2$, $NiCl_2$ or $CuCl_2$ for 1 h. After the incubation, cells were washed with 25 mM Tris pH 7.0 and 100 mM KCl and protein levels were determined. Samples were acid digested as described above and metal concentrations measured using furnace AAS.

Gene expression analysis

M. tuberculosis H37Rv wild-type cells in exponential phase in 7H9-OADC were cultured for 2 h with 100 μM Cu^{2+}, Zn^{2+}, Co^{2+}, Ni^{2+}, Mn^{2+} or Fe^{2+} as chloride salts, except for Zn^{2+} that was added in the sulphate form. Alternatively cells were exposed to 1 mM triclosan, a lipid metabolism inhibitor, nitroprusside, a nitrosative stressor, or the oxidative stressors TBHP, Paraquat, KCN. In alternative experiments, cells grown in Sauton's pretreated with Chelex (Sigma) (1 g/100 ml) were exposed to 10, 50 and 100 μM of Cu^{2+}, Zn^{2+}, Co^{2+} or Ni^{2+}. Cells were harvested, resuspended in 1 ml of TRIzol reagent (Invitrogen), and disrupted using lysing matrix B (MP Biomedicals) in a cell disrupter (FastPrep FP120, Qbiogene). RNA pellets were air dried and redissolved in 50 μl of diethyl pyrocarbonate-treated ultrapure water. Remaining DNA was removed with RNeasy minikit and an on-column DNase I kit (Qiagen). The RNA samples (1 μg) were used as templates for cDNA synthesis with random primers and SuperScript III reverse transcriptase (Invitrogen). Quantitative reverse transcription-PCR (qRT-PCR) was performed with iQ SYBR green supermix (Bio-Rad Laboratories), using primers listed in Table 2 and cycler conditions previously described (González-Guerrero *et al*., 2010). The RNA polymerase sigma factor (*sigA*) was used as an internal reference. Determinations were carried out with RNA extracted from three independent biological samples, with the threshold cycle (Ct) determined in triplicate. The relative levels of transcription were calculated by using the $2^{-\Delta\Delta Ct}$ method (Livak and Schmittgen, 2001). The mock reverse transcription reactions, containing RNA and all reagents except reverse transcriptase, confirmed that the results obtained were not due to contaminating genomic DNAs (data not shown). *ctpD* expression in the *ctpJ* mutant, and vice versa *ctpJ* expression in *ctpD* mutant cells, were measured in cells treated in similar manner.

Acknowledgements

This work was supported by NIH awards F32A1093049 (J.E.L.), 1R21AI082484 (J.M.A.), AI064282 (C.M.S.) and the Howard Hughes Medical Institute (C.M.S.).

References

Aderem, A., and Underhill, D.M. (1999) Mechanisms of phagocytosis in macrophages. *Annu Rev Immunol* **17:** 593–623.

Agnihotri, G., and Liu, H.W. (2003) Enoyl-CoA hydratase. Reaction, mechanism, and inhibition. *Bioorg Med Chem* **11:** 9–20.

Akif, M., Khare, G., Tyagi, A.K., Mande, S.C., and Sardesai, A.A. (2008) Functional studies of multiple thioredoxins from *Mycobacterium tuberculosis*. *J Bacteriol* **190:** 7087–7095.

Argüello, J.M. (2003) Identification of ion-selectivity determinants in heavy-metal transport P_{1B}-type ATPases. *J Membr Biol* **195:** 93–108.

Argüello, J.M., Eren, E., and González-Guerrero, M. (2007) The structure and function of heavy metal transport P_{1B}-ATPases. *Biometals* **20:** 233–248.

Argüello, J.M., González-Guerrero, M., and Raimunda, D. (2011) Bacterial transition metal P_{1B}-ATPases: transport mechanism and roles in virulence. *Biochemistry* **50:** 9940–9949.

Botella, H., Peyron, P., Levillain, F., Poincloux, R., Poquet, Y., Brandli, I., *et al*. (2011) Mycobacterial P_1-type ATPases mediate resistance to zinc poisoning in human macrophages. *Cell Host Microbe* **10:** 248–259.

Bradford, M.M. (1976) A rapid and sensitive method for the quantitation of microgram quantities of protein utilizing the principle of protein-dye binding. *Anal Biochem* **72:** 248–254.

Campbell, D.R., Chapman, K.E., Waldron, K.J., Tottey, S., Kendall, S., Cavallaro, G., *et al*. (2007) Mycobacterial cells have dual nickel-cobalt sensors: sequence relationships and metal sites of metal-responsive repressors are not congruent. *J Biol Chem* **282:** 32298–32310.

Cavet, J.S., Meng, W., Pennella, M.A., Appelhoff, R.J., Giedroc, D.P., and Robinson, N.J. (2002) A nickel-cobalt-sensing ArsR-SmtB family repressor. Contributions of cytosol and effector binding sites to metal selectivity. *J Biol Chem* **277:** 38441–38448.

Ehrt, S., and Schnappinger, D. (2009) Mycobacterial survival strategies in the phagosome: defence against host stresses. *Cell Microbiol* **11:** 1170–1178.

Eren, E., and Arguello, J.M. (2004) Arabidopsis HMA2, a divalent heavy metal-transporting P_{1B}-type ATPase, is involved in cytoplasmic Zn^{2+} homeostasis. *Plant Physiol* **136:** 3712–3723.

Feinbaum, R.L., Urbach, J.M., Liberati, N.T., Djonovic, S., Adonizio, A., Carvunis, A.R., and Ausubel, F.M. (2012) Genome-wide identification of *Pseudomonas aeruginosa* virulence-related genes using a *Caenorhabditis elegans* infection model. *PLoS Pathog* **8:** e1002813.

Flynn, J.L., and Chan, J. (2001) Immunology of tuberculosis. *Annu Rev Immunol* **19:** 93–129.

Forbes, J.R., and Gros, P. (2001) Divalent-metal transport by NRAMP proteins at the interface of host-pathogen interactions. *Trends Microbiol* **9:** 397–403.

González-Guerrero, M., Raimunda, D., Cheng, X., and Argüello, J.M. (2010) Distinct functional roles of homologous Cu^+ efflux ATPases in *Pseudomonas aeruginosa*. *Mol Microbiol* **78:** 1246–1258.

Hassani, B.K., Astier, C., Nitschke, W., and Ouchane, S. (2010) CtpA, a copper-translocating P-type ATPase involved in the biogenesis of multiple copper-requiring enzymes. *J Biol Chem* **285:** 19330–19337.

Hood, M.I., and Skaar, E.P. (2012) Nutritional immunity: transition metals at the pathogen-host interface. *Nat Rev Microbiol* **10:** 525–537.

van Kessel, J.C., and Hatfull, G.F. (2007) Recombineering in *Mycobacterium tuberculosis*. *Nat Methods* **4:** 147–152.

Lanzetta, P.A., Alvarez, L.J., Reinach, P.S., and Candia, O.A. (1979) An improved assay for nanomole amounts of inorganic phosphate. *Anal Biochem* **100:** 95–97.

Livak, K.J., and Schmittgen, T.D. (2001) Analysis of relative gene expression data using real-time quantitative PCR and the $2^{(-\Delta\Delta C(T))}$ method. *Methods* **25:** 402–408.

McLaughlin, H.P., Xiao, Q., Rea, R.B., Pi, H., Casey, P.G., Darby, T., *et al*. (2012) A putative P-type ATPase required for virulence and resistance to haem toxicity in *Listeria monocytogenes*. *PLoS ONE* **7:** e30928.

Mandal, A.K., Cheung, W.D., and Arguello, J.M. (2002) Characterization of a thermophilic P-type Ag^+/Cu^+-ATPase from the extremophile *Archaeoglobus fulgidus*. *J Biol Chem* **277:** 7201–7208.

Mawuenyega, K.G., Forst, C.V., Dobos, K.M., Belisle, J.T., Chen, J., Bradbury, E.M., *et al*. (2005) *Mycobacterium tuberculosis* functional network analysis by global subcellular protein profiling. *Mol Biol Cell* **16:** 396–404.

Osman, D., and Cavet, J.S. (2008) Copper homeostasis in bacteria. *Adv Appl Microbiol* **65:** 217–247.

Osman, D., Waldron, K.J., Denton, H., Taylor, C.M., Grant, A.J., Mastroeni, P., *et al*. (2010) Copper homeostasis in *Salmonella* is atypical and copper-CueP is a major periplasmic metal complex. *J Biol Chem* **285:** 25259–25268.

Osman, D., Patterson, C.J., Bailey, K., Fisher, K., Robinson, N.J., Rigby, S.E., and Cavet, J.S. (2013) The copper supply pathway to a *Salmonella* Cu,Zn-superoxide dismutase (SodCII) involves P_{1B}-type ATPase copper efflux and periplasmic CueP. *Mol Microbiol* **87:** 466–477.

Padilla-Benavides, T., Long, J.E., Raimunda, D., Sassetti, C.M., and Arguello, J.M. (2013) A novel P_{1B}-type Mn^{2+}-transporting ATPase is required for secreted protein metallation in *Mycobacteria*. *J Biol Chem* **288:** 11334–11347.

Pick, U. (1982) The interaction of vanadate ions with the Ca-ATPase from sarcoplasmic reticulum. *J Biol Chem* **257:** 6111–6119.

Raimunda, D., González-Guerrero, M., Leeber, B.W., 3rd, and Argüello, J.M. (2011) The transport mechanism of bacterial Cu^+-ATPases: distinct efflux rates adapted to different function. *Biometals* **24:** 467–475.

Raimunda, D., Long, J.E., Sassetti, C.M., and Argüello, J.M. (2012a) Role in metal homeostasis of CtpD, a Co^{2+} transporting P_{1B4}-ATPase of *Mycobacterium smegmatis*. *Mol Microbiol* **84:** 1139–1149.

Raimunda, D., Subramanian, P., Stemmler, T., and Arguello, J.M. (2012b) A tetrahedral coordination of Zinc during transmembrane transport by P-type Zn^{2+}-ATPases. *Biochim Biophys Acta* **1818:** 1374–1377.

Rensing, C., Fan, B., Sharma, R., Mitra, B., and Rosen, B.P. (2000) CopA: an *Escherichia coli* Cu(I)-translocating P-type ATPase. *Proc Natl Acad Sci USA* **97:** 652–656.

Rosadini, C.V., Gawronski, J.D., Raimunda, D., Argüello, J.M., and Akerley, B.J. (2011) A novel zinc binding system, ZevAB, is critical for survival of nontypeable *Haemophilus influenzae* in a murine lung infection model. *Infect Immun* **79:** 3366–3376.

Rowland, J.L., and Niederweis, M. (2012) Resistance mechanisms of *Mycobacterium tuberculosis* against phagosomal copper overload. *Tuberculosis (Edinb)* **92:** 202–210.

Rutherford, J.C., Cavet, J.S., and Robinson, N.J. (1999) Cobalt-dependent transcriptional switching by a dual-effector MerR-like protein regulates a cobalt-exporting variant CPx-type ATPase. *J Biol Chem* **274:** 25827–25832.

Sassetti, C.M., and Rubin, E.J. (2003) Genetic requirements for mycobacterial survival during infection. *Proc Natl Acad Sci USA* **100:** 12989–12994.

Studier, F.W. (2005) Protein production by auto-induction in high density shaking cultures. *Protein Expr Purif* **41:** 207–234.

Tottey, S., Rich, P.R., Rondet, S.A.M., and Robinson, N.J. (2001) Two Menkes-type ATPases supply copper for photosynthesis in *Synechocystis* PCC 6803. *J Biol Chem* **276:** 19999–20004.

Vergne, I., Chua, J., Singh, S.B., and Deretic, V. (2004) Cell biology of mycobacterium tuberculosis phagosome. *Annu Rev Cell Dev Biol* **20:** 367–394.

Wagner, D., Maser, J., Lai, B., Cai, Z., Barry, C.E., 3rd, Honer Zu Bentrup, K., *et al*. (2005) Elemental analysis of *Mycobacterium avium*-, *Mycobacterium tuberculosis*-, and *Mycobacterium smegmatis*-containing phagosomes indicates pathogen-induced microenvironments within the host cell's endosomal system. *J Immunol* **174:** 1491–1500.

Wagner, D., Maser, J., Moric, I., Vogt, S., Kern, W.V., and Bermudez, L.E. (2006) Elemental analysis of the *Mycobacterium avium* phagosome in Balb/c mouse macrophages. *Biochem Biophys Res Commun* **344:** 1346–1351.

Ward, S.K., Abomoelak, B., Hoye, E.A., Steinberg, H., and Talaat, A.M. (2010) CtpV: a putative copper exporter required for full virulence of *Mycobacterium tuberculosis*. *Mol Microbiol* **77:** 1096–1110.

Williams, E.P., Lee, J.H., Bishai, W.R., Colantuoni, C., and Karakousis, P.C. (2007) *Mycobacterium tuberculosis* SigF regulates genes encoding cell wall-associated proteins and directly regulates the transcriptional regulatory gene *phoY1*. *J Bacteriol* **189:** 4234–4242.

Zielazinski, E.L., Cutsail, G.E., 3rd, Hoffman, B.M., Stemmler, T.L., and Rosenzweig, A.C. (2012) Characterization of a cobalt-specific P1B-ATPase. *Biochemistry* **51:** 7891–7900.

Supporting information

Additional supporting information may be found in the online version of this article at the publisher's web-site.